CAAP Quarterly Report

[06/29/2023]

Project Name: "All-in-One Multifunctional Cured-In-Place Structural Liner for Rehabilitating of Aging Cast Iron Pipelines"

Contract Number: 693JK32250009CAAP

Prime University: North Dakota State University

Prepared By: [Ying Huang, ying.huang@ndsu.edu, 701-231-7651]

Reporting Period: [04/01/2023 – 07/01/2023]

Project Activities for Reporting Period:

In the 2nd quarterly report, Tasks 2.1, 3.1, 3.3 and 3.4 were carried out as proposed. In this quarter (Quarter 3), the research team has consistent progress on Tasks 2.1, 3.1, 3.3, and 3.4, and also conducted study on Task 4.1. The summaries of the key activities completed during the third reporting period are provided below.

Task 2.1 Preparation of Vitrimer Epoxy Resins, characterization, and optimization of the processing and curing conditions (20%): During this reporting period, the research team (Dr. Long Jiang and Austin Knight, Ph. D. student from NDSU) performed a new modified formation for self-healing polymer to overcome the limitations of the high-temperature requirements and long curing duration that needed to in the formation method presented in last report. The improved method uses methacrylic acid (MAA) to react with the epoxy directly forming a dimethacrylate using a commercial epoxy. The reaction mechanisms and formation developments are summarized below:

(1) Reaction Mechanisms of DTER Capable UV-Curable Epoxy Resins: The dynamic transesterification (DTER) mechanism is a common method used to give thermosets the ability to self-heal and to be recycled, as well as other vitrimer properties. In this work, this is accomplished by incorporating ester bonds and hydroxyl groups into the polymer through the reaction between an epoxy and an anhydride or a carboxylic acid. Last quarter, glutaric anhydride (GA) was ring-opened using glycerol and 2-hydroxyethyl acrylate (2-HEA) to introduce UV-curable acrylate groups into the resin. This was unsuccessful at synthesizing a UV-curable resin due to the high temperatures and times (190°C for >1 hr) needed to fully react the epoxy and resultant carboxylic acid from the anhydride ring-opening. For this reason, after UV-curing, the samples would need to undergo a thermal post-curing process. For this reason, after UV-curing, the samples would need to undergo a thermal post-curing process. During this quarter, rather than having 2-HEA ring-open the anhydride and the resultant carboxylic acid cure the epoxy, methacrylic acid (MAA) (with both a carboxylic acid and methacrylate functional group) was reacted with the epoxy directly forming a dimethacrylate using a commercial epoxy, bisphenol a diglycidyl ether (BADGE) (Figure 1). This is a simple reaction scheme that forms a more crosslink dense methacrylate resin that can be UV-cured.

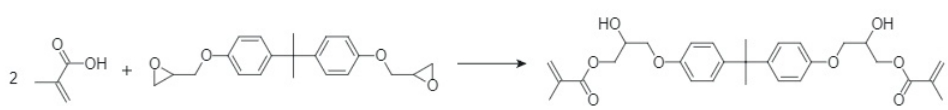

Figure 1. MAA reacting with BADGE to form a dimethacrylate.

(2) Procedure and Methods to Prepare DTER Capable UV-Curable Epoxy Resins: Three types of formulations were prepared 1) BADGE and MAA were mixed in an equal epoxide to carboxylic

acid functional group ratio, 2) To speed up the BADGE and MAA reaction, a catalyst was introduced at a concentration equal to 10% of the epoxide/carboxylic acid groups, and 3) the catalyst's concentration was minimized to 1% to study its impact at a lower concentration.

(3) Results: The first formation method was checked after 0.5, 3.5, 5.0, 7.0, and 8.5 hours of heating and the samples got progressively stronger but even after 8.5 hours the sample was not completely transparent. In the second mixing method, the high catalyst loadings proved to be an issue due to it also catalyzing the methacrylate polymerization reaction leading to the formation of a high-viscosity polymeric goo after 5 minutes at 90°C and 15 minutes at 70°C. After 10 minutes at 70°C, the resin could be diluted with a reactive diluent, and UV cured into a strong and mostly transparent sample, but the partial polymerization of the resin made it difficult to work with. In the third mixing method, to prevent premature polymerization of the methacrylate groups, the catalyst loading was reduced to 1 catalyst molecule for every 100 epoxide/carboxylic acid groups (~1%). This formulation was heated at 90°C and tested at 10, 15, and 20 minutes. After 20 minutes of heating, the UV-cured samples were completely transparent and very strong (Figure 2). The resin also had a relatively low viscosity and did not experience premature methacrylate polymerization. After this initial reaction, the same reactive diluent can be added to reduce the viscosity and more catalyst can be added to help with the DTER mechanism.

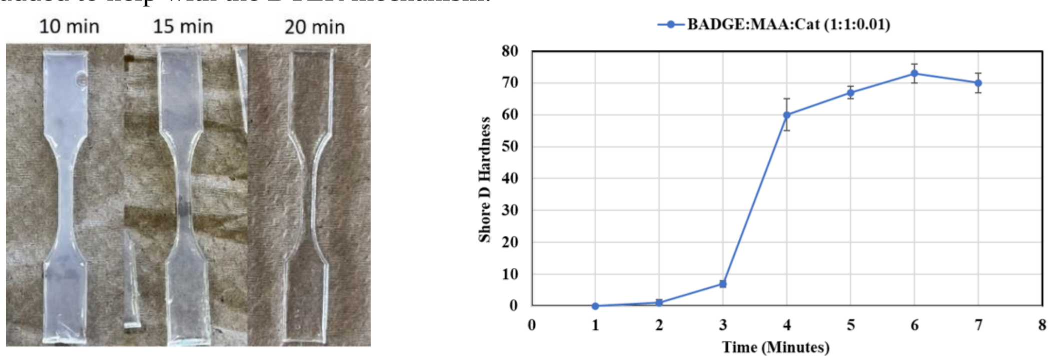

(a) (b)

Figure 2. (a) Transparency, and (b) curing process of the self-healing polymer fabricated by the third formation.

(4) Characterization of Curing Rate for the Third Formation: After determining a satisfactory formulation, the curing rate was determined by measuring the hardness of samples after increasing UV-curing times (Figure 2(b)). After 4 minutes the formulation had cured the entire thickness and after 5 to 6 minutes the sample reached its maximum hardness.

Task 3.1 High Mechanical Performance (10%): During this reporting period, the research team (Dr. Ying Huang, Dr. Zhibin Lin, Dr. Xingyu Wang, Tofatun Jannet, Ph. D. student, Colby Rance and Kathryn Quenettee, sophomore students from NDSU) conducted experimental studies on nanoparticle reinforcement, including rheology properties, micro-structure analysis, and damage tolerance. All of these properties are directly related to the mechanical properties of the nanocomposite; and the findings have enriched the research team's understanding of nanoparticle reinforcement and can also be essential in guiding the design of the nanocomposite. The investigations and their key findings are provided below:

(1) Influence of Nanoparticles on the Rheology Properties of Nanocomposite: Rheological behavior of epoxy is of great importance as it has a significant impact on the processing, performance, and practical applications of polymeric materials. Figure 3 shows the viscosity profiles of neat epoxy and three nanoparticle reinforced epoxy as a function of shear rate. Influence of different shapes of nanoparticles: among the three types of nanoparticles, CNTs showed the most significant influence in the rheological properties among the three nanoparticles, due to their high aspect ratio and unique

tubular structure. GNPs also increased the viscosity of the nanocomposite fluid but were less than CNTs, their larger surface area also provided strong interaction with the epoxy fluid. On the other hand, there was no obvious difference between the viscosity of neat epoxy and ND (0-D) reinforced epoxy due to the superior dispersion quality of ND. Their spherical shape and smaller size led to lesser interaction with the base fluid, resulting in less significant changes in the rheological properties.

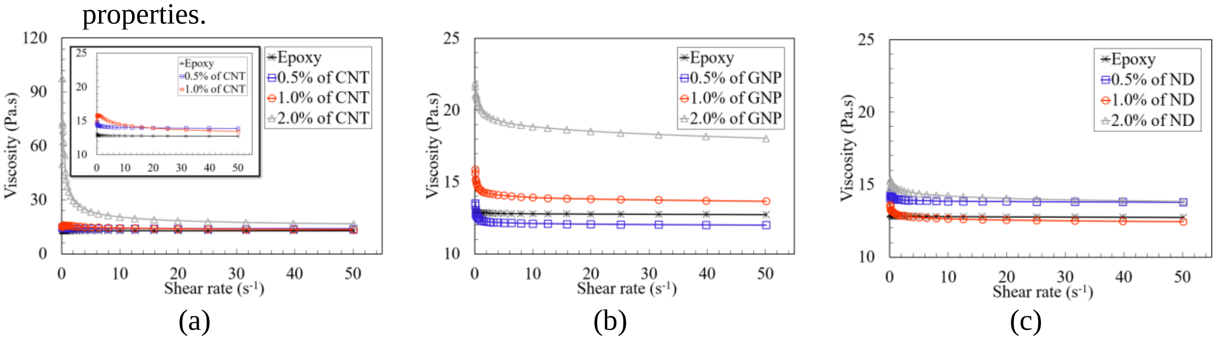

Figure 3. Viscosity profiles of neat epoxy and nanoparticle reinforced epoxy as a function of shear rate.

(2) Influence of Nanoparticles on the Microstructure of Nanocomposites: In this study, micro-CT was utilized to gain insights into the voids and defects within the nanocomposite. The results demonstrate that the incorporation of nanoparticles significantly impacts the microstructure nanocomposites and aids in reducing the void content. Figure 4 displays the reconstructed 3-D image of the epoxy by Micro-CT as a demonstration, while the cross-sections of the nanocomposite were presented in Figure 5. Carbon Nanotubes (CNTs, 1-D) demonstrated efficacy in reducing void percentage and size due to their tubular shape. However, at higher concentrations, a larger voids percentage was observed. Graphene Nanoplatelets (GNPs, 2-D) were particularly effective in void reduction, particularly at higher concentrations. Nanodiamonds (NDs, 0-D), due to their compact shape and small size, consistently reduced void size and percentage across all concentrations.

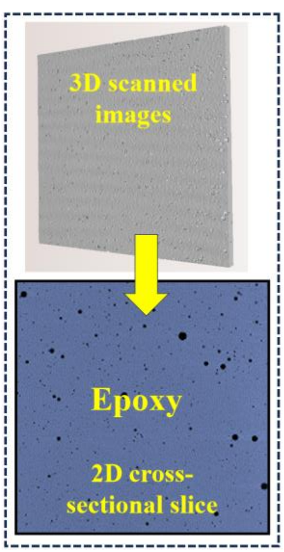

Figure 4. Micro-CT images of epoxy.

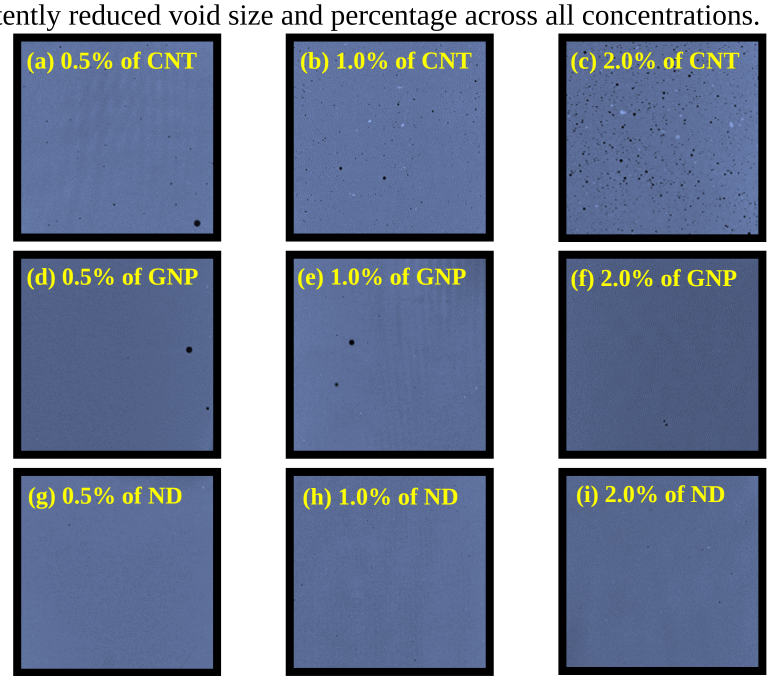

Figure 5. Cross-sectional Micro-CT images of nanocomposites.

Task 3.3. Reducing the Permeability and Investigating the Interfacial Bonding Chemical Analysis (15%): During this reporting period, the research team (Dr. Liangliang Huang, Qiuhao Chang, Ph. D. student from

University of Oklahoma) have conducted studies on developing computational models for the evaluating hydrogen models based on their density and self-diffusion properties.

(1) To assess the performance of different hydrogen models, we tested four models: two united models, and two 2-site models. The evaluation focused on comparing the predicted density and bulk self-diffusion properties at different temperatures. The results, presented in the tables and figure below, indicate that the united model exhibits satisfactory accuracy in predicting these properties in bulk hydrogen across varying temperatures and pressures. By systematically evaluating these hydrogen models, we can make an informed choice regarding the most suitable model for our future simulations of hydrogen permeability in self-healable epoxy resin. These findings provide a solid foundation for further investigations and design of molecular dynamics simulations to explore the behavior of hydrogen in the selected polymer systems.

Table 1. Density & Self-Diffusion Properties of Bulk Hydrogen at 1 atm.

T (K)	Experimental ρ (g/cm³)	Buch[1] *United Model*		Frost et al.[2] *United Model*		Cracknell[3] *Two-Site Model*		Yang & Zhong[4] *Two-Site Model*	
		ρ (g/cm³)	error	ρ (g/cm³)	error	ρ (g/cm³)	error	ρ (g/cm³)	error
90.3	2.72E-04	2.72E-04	***0.14%***	2.72E-04	***0.13%***	2.75E-04	***1.13%***	2.76E-04	***1.26%***
273	9.00E-05	8.99E-05	***0.02%***	9.01E-05	***0.14%***	9.06E-05	***0.80%***	9.01E-05	***0.22%***
293.2	8.38E-05	8.39E-05	***0.06%***	8.38E-05	***0.03%***	8.33E-05	***0.56%***	8.44E-05	***0.68%***

T (K)	Experimental D_S (cm²/s)	Buch[1] *United Model*		Frost et al.[2] *United Model*		Cracknell[3] *Two-Site Model*		Yang & Zhong[4] *Two-Site Model*	
		D_s (cm²/s)	error	D_s (cm²/s)	error	D_s (cm²/s)	error	D_s (cm²/s)	error
90.3	0.192	0.170	***11.23%***	0.174	***9.55%***	0.219	***14.15%***	0.211	***9.84%***
273	1.285	1.257	***2.16%***	1.278	***0.56%***	1.298	***1.00%***	1.183	***7.94%***
293.2	1.400	1.490	***6.39%***	1.395	***0.34%***	1.427	***1.93%***	1.352	***3.44%***

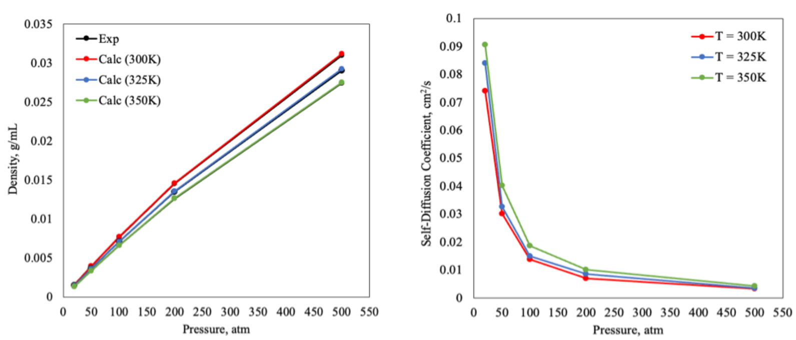

Figure 6. Density and Self-Diffusion of Bulk Hydrogen at Varying Temperatures and Pressures: United Model vs the Experimental Measurements.

Task 3.4 Finite Element Numerical Analysis to Guide the Design of the Developed high-performance Healable CIPP Structural Liner (20%): During this reporting period, the research team (Dr. Chengcehng Tao, Xiaoyue Zhang and Junyi Duan, Ph. D. students from Purdue University) have conducted computational modeling of CIPP liners for aged pipeline rehabilitation as summarized below:

(1) Methodology: A Finite Element Analysis (FEA) was implemented using ABAQUS CAE to model the restoration of damaged cast-iron pipes via CFRP liners, the created model is presented in Figure 7. To ensure the accuracy of the model, careful consideration was given to element types, boundary conditions, and mesh qualities. The model utilized 4-node shell (S4R) elements for both the pipeline and liner, and hinges at the ends for finite length simulation. To boost accuracy, finer mesh was employed around the corrosion hole. The model only accounted for in-pipe pressure, neglecting the soil loads. The study encompassed CFRP liner thicknesses from 0.5-8 mm, simulating pressure conditions of 1.0, 1.5, and 2.0 MPa. Finally, a linear elastic constitutive model was applied for the CFRP liner, while cast-iron was treated as elasto-plastic.

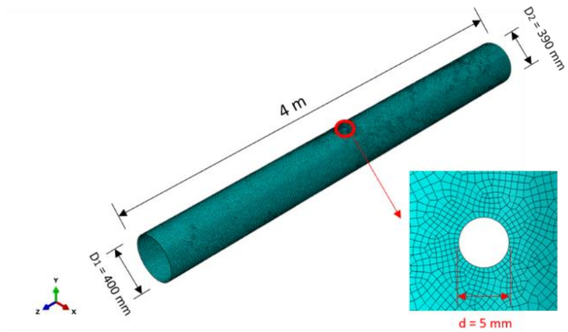

Figure 7. Geometry and mesh of the pipe-liner system. (D_1 – outer diameter of the cast-iron pipe; D_2 – outer diameter of the CFRP liner; d – diameter of the corrosion hole).

(2) Results and Discussion: The computational analysis of the pipe-liner shows the rehabilitation effect of CFRP liners with various thicknesses and in-pipe pressure on the mechanical responses of the damaged cast-iron pipes. Different thicknesses of CFRP liner (0 to 8 mm) are used to rehabilitate pipes with in-pipe pressure of 1.0, 1.5, and 2.0 MPa. Results in Figure 8 exhibited that stress and displacement of the cast-iron pipe decrease by the increased the liner thickness and decreased in-pipe pressure. The rehabilitation impact of the CFRP liner is notably apparent when the thickness is elevated from zero to 2mm. The FEA results indicated that implementing a CFRP liner and increasing its thickness can effectively enhance the structural integrity of the damaged cast-iron pipe.

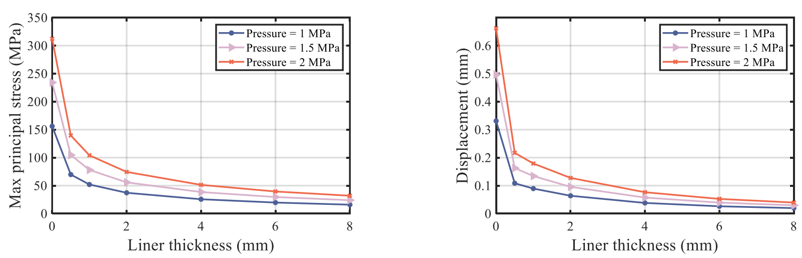

(a) (b)

Figure 8. Mechanical responses of the cast-iron pipe versus CFRP liner thickness under different in-pipe pressure conditions.

(3) Additionally, we conducted a parametric study and compared an undamaged cast-iron pipe with damaged cast-iron pipes rehabilitated by CFRP liners with different liner thicknesses. Figure 9(a) shows the maximum principal stress of the pipes. The red dashed line shows the response of the undamaged pipe under 1.5MPa without any rehabilitation, and the blue dot line shows the performance of damaged pipes rehabilitated by liners with different thicknesses. According to the figure, the rehabilitated damaged pipe with a 1.5 mm CFRP liner achieves a comparable performance to that of the undamaged one. Figure 9(b) depicts the stress nephogram of the damaged pipe without the liner, and Figure 9(c) shows the comparative analysis of the displacement of the pipe. It can be observed that the CFRP liner with a thickness of 2.5 mm has optimal performance in rehabilitating damaged cast-iron pipes.

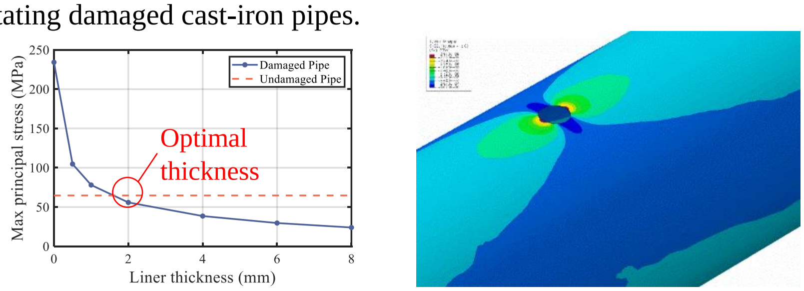

(a) (b)

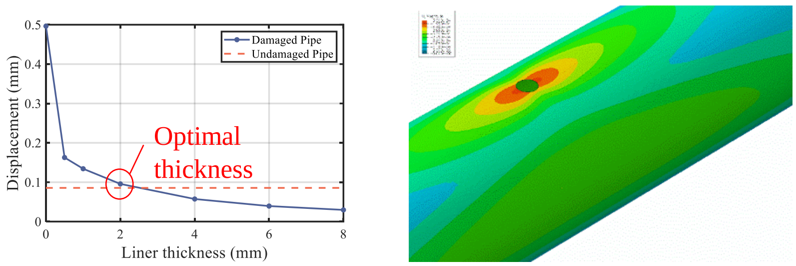

(c) (d)

Figure 9. Mechanical performance of the damaged pipe with FEA nephograms.

Task 4.1 Development of Embedded Distributed Fiber Optic Sensors for Self-sensing Structural Liner (10%): During this reporting period, the research team (Dr. Ying Huang and Dr. Xingyu Wang) conducted experimental studies on corporation distributed fiber optic sensors to polymeric composite, the major findings are presented below:

(1) This study investigated the incorporation of distributed optical fiber sensors into composite materials, specifically within structural liner systems. An optical sensor, embedded within a 100x13x3mm polymer specimen (Figure 10(a)), was utilized to monitor internal strain during the curing process. Knowledge of internal strain is crucial for detecting cure shrinkage and residual deformations, which can lead to residual stress, performance degradation, shape distortions, and severe complications such as matrix cracks and delamination. The study examined the internal residual strain produced during each curing cycle stage. The deployed sensors, with measurement points every 0.65mm, provide time-series strain development data. Figure 10(b) showcases the curing strain development over 14 days, depicting strain progression across the whole sample. The internal curing strain measurement can provide detailed curing process monitoring at each point, as illustrated in Figure 10(c). As shown in Figure 10(d), the findings highlighted potential vulnerability areas within the liner by showing strain development at each point, as these areas have high pre-stress from the curing reaction, are likely most susceptible to damage under operational conditions.

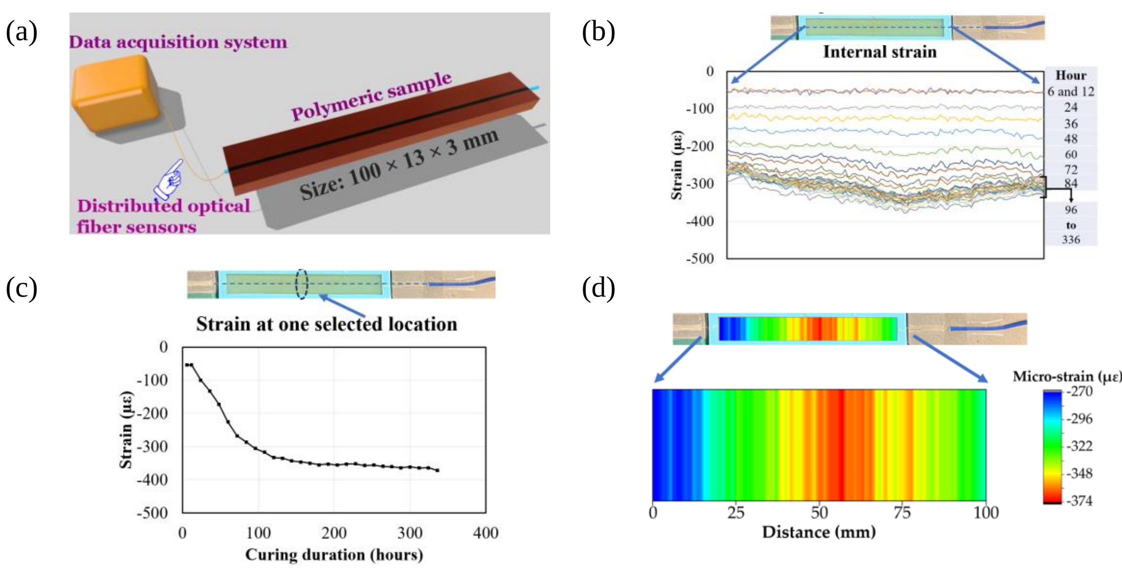

Figure 10. (a) Illutration of the polymer sample with distributed fiber optic sensors, (b) internal strain monitoring for 14 days, (c) strain development at one selected location, and (d) strain map after 14 days.

Project Financial Activities Incurred during the Reporting Period:

The cost breakdown during the reporting period in each category according to the budget proposal is shown in Table 2.

Table 2. Cost breakdown

Category	Amount spent during Q3
Personnel	
Faculty	$22,000
Postdoc	$6,000
Students (RA and UR)	$8,400
Benefits	$9,852
Operating Expenses	
Travel	$0
Materials and Supplies	$6,000
Recharge Center Fee	$3,000
Consultant Fee	$1,600
Subcontracts	Subawards issued
Indirect Costs	$245,584

Project Activities with Cost Share Partners:

The Match fund from NDSU for this project is coming from the tuition of the associated graduate students during their work on this project. During the reporting period (Q3), Austin Knight and Tofatun Jannet were hired on the project for summer. The tuition for the two students during Q3 is estimated to be $9,738 at a rate of $811.52 per credit.

Project Activities with External Partners:

During this reporting period, the project completed all the paperwork to hire the project consultant, George Ragula, the president and CEO of Rauglatech, who has 43 years of service in the gas industry, engineering, operations, construction (including trenchless), R&D and management. George started to participate regular team meeting and provide regular consultant services to the team.

Potential Project Risks:

- No potential risks were noticed during this reporting period.

Future Project Work:

In the next quarter, the research team will continue working on Tasks 2.1, 3.1, 3.3, 3.4, 4.1 and expand the work onto Tasks 2.2 and 3.2 whenever applicable.

Potential Impacts on Pipeline Safety:

The preliminary results on self-healing epoxy and high-performance nano-epoxy composites show the potential of the proposed materials, which can be used to enhance the safety of any pipelines which needs to use epoxy related materials.